

Large Brightness Variations of Uranus at Red and Near-IR Wavelengths

Richard W. Schmude Jr.
Gordon State College
419 College Dr., Barnesville, GA 30204 USA
schmude@gordonstate.edu

Ronald E. Baker
Indian Hill Observatory, Chagrin Valley Astronomical Society
PO Box 11, Chagrin Falls, OH 44022 USA
rbaker52@gmail.com

Jim Fox
Astronomical League and the AAVSO
P.O. Box 135, Mayhill, NM 88339
Makalii45@gmail.com

Bruce A. Krobusek
5950 King Hill Road, Farmington, NY, 14425, USA
bkrobusek@gmail.com

Anthony Mallama
14012 Lancaster Lane, Bowie, MD 20715 USA
anthony.mallama@gmail.com

2015 October 14

Pages, 30; tables, 10; figures, 13

Abstract

Uranus is fainter when the Sun and Earth are near its equatorial plane than when they are near the projection of its poles. The average of the absolute values of the sub-Earth and sub-Sun latitudes (referred to as the sub-latitude here) is used to quantify this dependency. The rates of change of magnitude with sub-latitude for four of the Johnson-Cousins band-passes are B-band, -0.48 ± 0.11 milli-magnitudes per degree; V-band, -0.84 ± 0.04 ; R-band, -5.33 ± 0.30 ; and I-band -2.79 ± 0.41 . Evaluated over the range of observed sub-latitudes, the blue flux changes by a modest 3% while the red flux varies by a much more substantial 30%. These disk-integrated variations are consistent with the published brightness characteristics of the North and South Polar Regions, with the latitudinal distribution of methane and with a planetary hemispheric asymmetry. Reference magnitudes and colors are also reported along with geometric albedos for the seven Johnson-Cousins band-passes.

Keywords:

Uranus, Uranus atmosphere, Photometry

1. Introduction

Uranus is the only planet in our solar system whose rotational axis is highly inclined to the ecliptic pole. This unique geometry permits favorable viewing of both high and low latitudes from the Earth. The passage of the Sun and Earth through the planet's equatorial plane in 2007 was observed closely. Unexpected storm activity (de Pater et al., 2015) and other atmospheric changes have been noted since the arrival of spring in the northern hemisphere.

At the same time, the planet has grown considerably brighter especially at red and near-IR wavelengths. In this paper we report on this post-equinox brightening and we analyze the historical record of standardized photometry extending back to the middle of the last century. The brightness changes are discussed in the context of disk-resolved Uranian imagery (Karkoschka, 2001b), spectrographic observations (Sromovsky et al., 2014) and characterization of the south polar region (Rages et al., 2004). This work is closely related to that of Lockwood and Jerzykiewicz (2006) who have recorded the brightness of Uranus in the b- and y-bands since 1972.

Section 2 summarizes a long series of b- and y-band photometry recorded by Lockwood and Jerzykiewicz and explains its relationship to our B- and V-band results. Section 3 provides an overview of the photometric and calibration techniques used to determine the magnitudes analyzed in this paper. Section 4 describes the small brightness changes that we and previous investigators observed in the B- and V-bands over 73% of a Uranian year and compares them to the expected change due to the planet's oblate figure. Section 5 describes the large brightness changes that were recorded in the R- and I-bands, which are being reported here for the first time. Section 6 examines the effects that the satellites, rings and clouds of Uranus might have on observed brightness. Section 7 discusses the variable planetary brightness in terms of the polar regions, methane depletion and hemispheric asymmetry. Section 8 lists reference magnitudes, colors and albedos. Section 9 summarizes our conclusions.

2. Related photometry in blue and yellow band-passes

The main subject of this paper is wide-band photometry of Uranus in visible and near-IR wavelengths. Before commencing on that discussion though, we summarize the important medium-band blue and yellow photometry of Lockwood and Jerzykiewicz (2006). This work has been updated on Lockwood's web page at http://www2.lowell.edu/users/wes/U_N_lcurves.pdf and now spans 42 years. The annual means of their b (472 nm) and y (551 nm) are plotted in Figs. 1 and 2 and they reveal quasi-sinusoidal variations peaking near the Uranian solstice of the 1980s. Lockwood notes that "The b amplitude slightly exceeds the expected 0.025 mag purely geometrical variation caused by oblateness as the planetary aspect changes, seen from Earth. The y amplitude is several times larger, indicating a strong equator-to-pole albedo gradient." This result anticipates the blue and green wide-band results which are presented in the present paper.

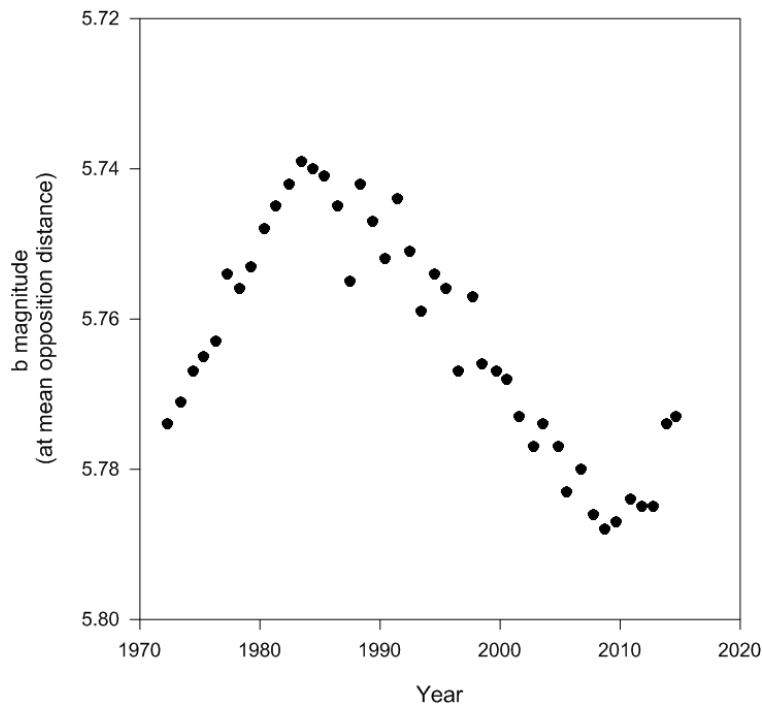


Fig. 1. The b-band variability of Uranus.

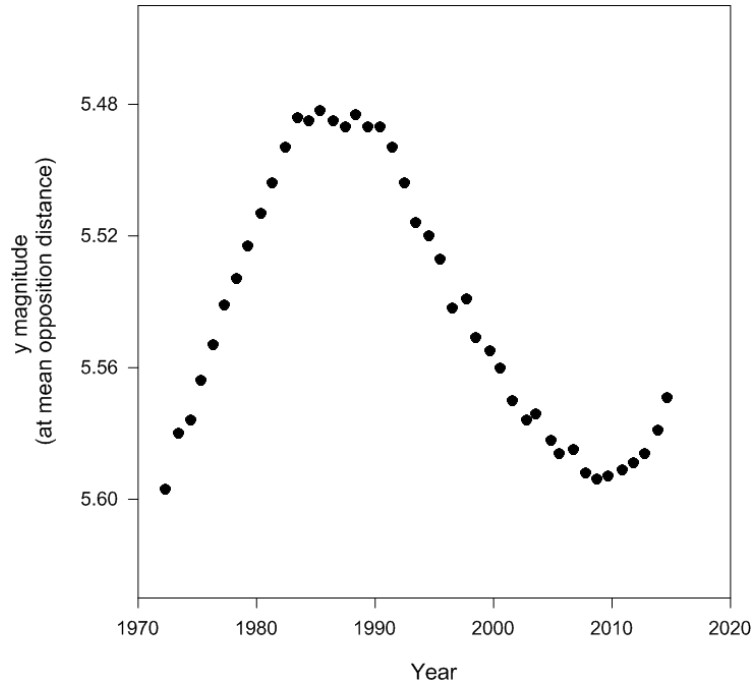


Fig. 2. The y-band variability of Uranus.

3. Photometry and calibrations

The magnitudes used in this study are on the Johnson-Cousins system. The original Johnson system was defined by Johnson et al. (1966) and the Cousins extension is described in Cousins (1976a and 1976b). The characteristics of the system are given in Table 1.

Table 1: Characteristics of the Johnson-Cousins systems

Filter	Effective Wavelength (μm)	FWHM (μm)
U	0.360	0.068
B	0.436	0.098
V	0.549	0.086
R	0.700	0.209
Rc	0.641	0.158
I	0.900	0.221
Ic	0.798	0.154

In order to sample the brightness of Uranus over a wide range of sub-Earth and sub-Sun latitudes we retrieved measurements dating back to the 1950s on the Johnson-Cousins magnitude system. The data sources are summarized in Table 2 and are described below.

Serkowski (1961) reports two sets of V and B-V magnitudes of Uranus made between October 30, 1953 and April 12, 1961 in his Table VIII. These values are corrected for extinction and color transformation (those corrections are described later in this section) but are not corrected for distance, phase and oblateness effects. One set is based on his system of primary standards and the other is based on his system of 10-year standards. The two sets of measurements have mean differences of 0.0025 and 0.001 magnitudes for the V and B-V sets. These are small and are assumed to be negligible. The data set based on primary standards is selected for this study because it contains more measurements. Each B value is the sum of the V and B-V value.

Jerzykiewicz and Serkowski (1966) reports V, B-V and B' magnitudes in their Table VI. We did not use their B' magnitudes because they are corrected for oblateness. The V and B-V values are used in this study. The B-V values are computed in the same way as in the Serkowski data set.

As a check on both studies, one of us (RWS) compared the measured V and B-V values of the Ten-Year Standards in Table VI of Serkowski (1961). Most of the values are consistent with those in Iriarte et al. (1965). Jerzykiewicz and Serkowski (1966) report that the Ten-Year Standard star Xi-Boötis varied by over 0.03 magnitudes in 1964. Sinnott and Perryman (1997) list this star as a variable changing by less than 0.1 magnitude. All of the other Ten-Year Standards are listed as having a constant brightness by Sinnott and Perryman (1997). This leads us to believe that the work of Serkowski (1961) and of Jerzykiewicz and Serkowski (1966) are of high quality.

Schmude (1992, 1993, 1994, 1996, 1997a, 1997b, 1998a, 1998b, 2000a, 2000b, 2001, 2002, 2004, 2005, 2006a, 2006b, 2008, 2009, 2010a, 2010b, 2012, 2013, 2014, 2015a and 2015b) and co-workers report V filter results for Uranus. In many cases, B, R and I results are also reported. All values are corrected for extinction. Data in 1997 and from 1999 and later were corrected for color transformation in the original reports. Therefore, no further modification was made to these data. The values collected from 1991-1995 and 1997 in Schmude (1992, 1993, 1994, 1996, 1997a, b, 1998b) were not corrected for color transformation in the original reports. Therefore, corrections were made before adding these measurements to the data set used in this study. The transformation coefficients were computed from the two-star method outlined in Hall and Genet (1988, p. 186). Between 1991 and 1999, the same photometer was used. In cases where there was no transformation data available, the data was not included in the current study. Starting in 1999, RWS used a new photometer and thus re-measured the transformation coefficients (Schmude, 2000b). Others besides RWS and JF contributed brightness measurements to this data set. Their names are listed in the original sources along with their transformation coefficients. The complete data set is available upon request from one of the authors (RWS).

New photometry acquired by two of the authors (BAK and REB) is summarized in Table 2 and the observations themselves are listed in Tables 3 and 4. Uncertainties for the observations by BAK and REB are listed with their observations. Formal error bars are not available for the other observations but they are estimated to be a few hundredths of a magnitude or less.

Table 2: Data sets used in the development of the photometric model of Uranus

Years	Filters	Source
1953-1961	B V	Serkowski (1961)
1962-1966	B V	Jerzykiewicz and Serkowski (1966)
1991-2015	B V R I	Schmude (1992, 1993, 1994, 1996, 1997a, b, 1998a, b, 2000a, b, 2001, 2002, 2004, 2005, 2006a, b, 2008, 2009, 2010a, b, 2012, 2013, 2014 and 2015a, b)
2013-2014	B V R I	Krobusek (this paper)
2014	B V Rc Ic	Baker (this paper)

Table 3: Magnitudes recorded by BAK

MJD*	B	+/-	V	+/-	R	+/-	I	+/-
56626.02	-6.605	0.014	-7.135	0.014	-6.824	0.022	-5.663	0.046
56626.08	-6.598	0.020	-7.140	0.019	-6.897	0.020	-5.675	0.047
56643.98	-6.629	0.013	-7.127	0.013	-6.915	0.032	-5.700	0.089
56888.32	-6.613	0.017	-7.128	0.016	-6.920	0.032	-5.696	0.089
56894.29	-6.625	0.017	-7.183	0.019	-6.947	0.035	-5.706	0.091
56895.28	-6.609	0.030	-7.178	0.016	-6.918	0.035	-5.770	0.085

*Modified Julian Date

"+/-" refers to uncertainty

Table 4: Magnitudes recorded by REB

MJD*	B	+/-	V	+/-	Rc	+/-	Ic	+/-
56876.37	-6.620	0.008	-7.113	0.008	-6.987	0.022	-6.085	0.047
56876.38	-6.594	0.006	-7.112	0.007	-6.985	0.023	-6.073	0.048
56924.26	-6.618	0.006	-7.134	0.008	-6.991	0.023	-6.085	0.048
56924.27	-6.627	0.007	-7.127	0.007	-7.016	0.023	-6.077	0.049
56942.23	-6.623	0.006	-7.128	0.007	-6.995	0.022	-6.086	0.048
56942.24	-6.630	0.009	-7.137	0.010	-7.002	0.023	-6.076	0.048

*Modified Julian Date

"+/-" refers to uncertainty

The observations were made differentially with respect to standard stars of the Johnson-Cousins system. The procedures for differential photometry were described by Hardie (1962) and again by Hall and Genet (1988).

All magnitudes were corrected for extinction and color effects. The extinction correction accounts for dimming due to the Earth's atmosphere by applying a correctional coefficient to the air mass through which the object was viewed. Color correction takes the 'natural' magnitudes recorded by the hardware and converts them to standard magnitudes on the Johnson-Cousins system. Equations 1 and 2 illustrate extinction correction and color transformation, respectively.

$$m_0 = m - k_M X \tag{1}$$

$$M = m_0 + \epsilon C \tag{2}$$

In equation 1, m is the raw magnitude, k_M is the extinction coefficient, X is the air mass and m_0 is the magnitude corrected for extinction. In equation 2, ϵ is the transformation coefficient, C is the color index and M is the magnitude corrected for extinction and color. More information on photometric correction can be found in Hall and Genet (1988) and in Hardie (1962).

A concern with regard to color transformation is that color coefficients are based on stellar spectra. However, planetary spectra are different and that of Uranus, in particular, is quite steep at long wavelengths as seen in Fig. 3.

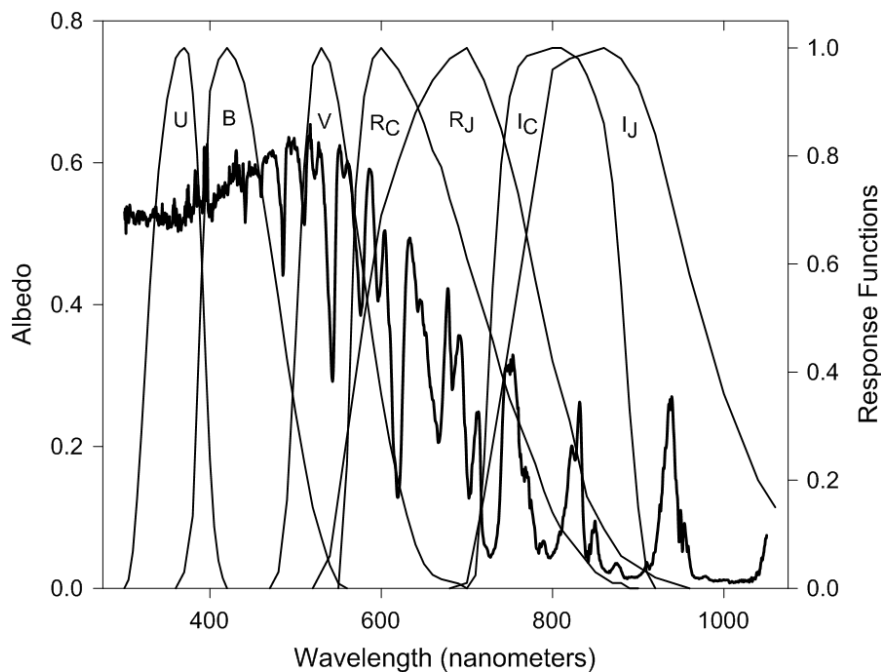


Fig. 3. The response functions of the Johnson-Cousins system (Filter Profile Service at <http://skyservice.pha.jhu.edu>) are superposed on the albedo of Uranus (Karkoschka, 1998).

After extinction correction and color transformation, the magnitudes were reduced to a standard distance of one astronomical unit from the Earth to Uranus and from the Sun to Uranus.

The phase angle of Uranus can only be as large as three degrees, so its effect on the planet's magnitude is expected to be very small. In order to estimate the size, we evaluated the phase functions of Jupiter in U, B, V, R and I (Mallama and Schmutte, 2012) and of Venus in B, V, R and I (Mallama et al., 2006) at the three degree limit for Uranus. In all cases the magnitude change is 0.01 magnitude or less. Likewise, Lockwood and Thompson (2009) found that the phase function for Titan is well under 0.01 magnitude per degree. These results are all consistent with results reported by Lockwood (1978) that the effect of solar phase angle is less than 0.003 magnitude. Thus, the effect of solar phase angle on the brightness of Uranus is not significant and, since the exact phase function is not known, no correction was applied. Likewise, no correction was made for oblateness but that effect will be discussed later in the paper. Finally, to conclude this section, mean magnitudes for each opposition are listed in Table 5.

Table 5: Mean magnitude and number of observations for each opposition

Year	B	#	V	#	R	#	I	#	Rc	#	Ic	#
1954.04	-6.583	11	-7.126	11	----	0	----	0	----	0	----	0
1955.05	-6.632	6	-7.165	6	----	0	----	0	----	0	----	0
1956.06	-6.621	18	-7.150	18	----	0	----	0	----	0	----	0
1957.07	-6.611	12	-7.133	12	----	0	----	0	----	0	----	0
1958.08	----	0	----	0	----	0	----	0	----	0	----	0
1959.10	-6.624	10	-7.146	10	----	0	----	0	----	0	----	0
1960.11	-6.601	17	-7.130	17	----	0	----	0	----	0	----	0
1961.12	-6.605	8	-7.131	8	----	0	----	0	----	0	----	0
1962.13	-6.597	15	-7.120	15	----	0	----	0	----	0	----	0
1963.14	----	0	----	0	----	0	----	0	----	0	----	0
1964.16	-6.587	2	-7.095	2	----	0	----	0	----	0	----	0
1965.17	-6.606	8	-7.099	8	----	0	----	0	----	0	----	0
1966.18	-6.610	13	-7.094	13	----	0	----	0	----	0	----	0
1991.48	-6.626	14	-7.178	49	----	0	----	0	----	0	----	0
1992.50	-6.584	20	-7.162	29	----	0	----	0	----	0	----	0
1993.51	-6.691	34	-7.153	34	-6.995	19	-5.749	19	----	0	----	0
1994.52	-6.667	15	-7.156	16	-6.962	13	-5.712	13	----	0	----	0
1995.53	-6.619	7	-7.175	8	-6.997	7	-5.684	7	----	0	----	0
1996.54	----	0	-7.120	12	----	0	----	0	----	0	----	0
1997.56	----	0	-7.148	53	----	0	----	0	----	0	----	0
1998.57	-6.657	10	-7.156	41	----	0	----	0	----	0	----	0
1999.58	-6.647	20	-7.157	30	-6.890	1	-5.600	1	----	0	----	0
2000.59	-6.560	1	-7.143	12	-6.821	9	-5.611	19	----	0	----	0
2001.60	-6.604	5	-7.131	74	-6.930	1	----	0	----	0	----	0
2002.62	-6.628	8	-7.128	34	-6.747	7	-5.553	3	----	0	----	0
2003.63	-6.595	15	-7.123	20	----	0	----	0	----	0	----	0

2004.64	-6.618	5	-7.111	10	-6.678	4	----	0	----	0	----	0
2005.65	-6.659	11	-7.120	22	----	0	----	0	----	0	----	0
2006.66	-6.596	5	-7.113	45	-6.680	1	----	0	----	0	----	0
2007.68	-6.645	17	-7.124	32	-6.707	3	----	0	----	0	----	0
2008.69	-6.658	7	-7.118	58	----	0	----	0	----	0	----	0
2009.70	-6.650	2	-7.150	4	----	0	----	0	----	0	----	0
2010.71	-6.555	26	-7.134	27	-6.775	4	-5.613	3	----	0	----	0
2011.72	-6.576	17	-7.141	18	-6.814	5	-5.697	4	----	0	----	0
2012.74	-6.645	22	-7.116	24	-6.812	6	-5.628	5	----	0	----	0
2013.75	-6.651	38	-7.125	41	-6.879	3	-5.679	3	----	0	----	0
2014.76	-6.630	40	-7.134	40	-6.928	3	-5.724	3	-6.996	6	-6.080	6

4. Brightness variations in the B and V bands

The B- and V-band observations span the years from 1953 through 2015 and include two equinoxes. The brightness changes during this time interval are shown in Figs. 4 and 5. Dimming is evident near the 1966 and 2007 equinoxes (MJDs 39300 and 54300, respectively).

We computed a value called the *sub-latitude*, which is the average of the absolute values of the planetographic sub-Earth and sub-Sun latitudes, for the time of each observed magnitude.

Since Uranus orbits at a distance of about 20 AU the sub-latitude, sub-Earth latitude and sub-Sun latitude are nearly equal.

The relationships between magnitudes and sub-latitude are shown in Figs. 6 and 7, and they are quantified in Table 6. The change of magnitude per degree of latitude for the northern and southern hemispheres combined (black lines in the figures) is -0.48×10^{-3} in the B-band and -0.84×10^{-3} in the V-band.

When the data are separated by the hemisphere of the sub-latitude (orange and green symbols and lines in Figs. 6 and 7) they imply the planet was brighter when southern latitudes were centered on the disk in both bands.

The oblate figure of Uranus causes the apparent surface area of its disk to increase along with sub-latitude. The excess over the area projected at sub-latitude zero is proportional to sine-squared of the sub-latitude. Since the ratio of the planet's equatorial radius to its polar radius is 1.0235, the excess is 0.0235 at 90 degrees. Fig. 8 shows the observed excess flux of Uranus plotted versus the sine-squared term in the B-band and V-bands along with best-fitting lines in color. The black lines indicate the geometrical relationship between surface area and oblateness. The observed slope for the V-band (0.0575 ± 0.0030) exceeds the slope for oblateness (0.0235) by more than 10 standard deviations. However, the observed slope for the B-band (0.0330 ± 0.0070) only exceeds the oblateness slope by about 1.3 standard deviations. Thus our results for the B- and V-bands are in general agreement with those of Lockwood and Jerzykiewicz (2006) for the b- and y-bands.

Table 6. Magnitude as a function of sub-latitude

Band	Zero Point	+/-	Slope*	+/-
B	-6.61	0.02	-0.48	0.11
V	-7.11	0.02	-0.84	0.04
R	-6.69	0.02	-5.33	0.30
I	-5.57	0.02	-2.79	0.41

* Milli-magnitudes per degree of latitude

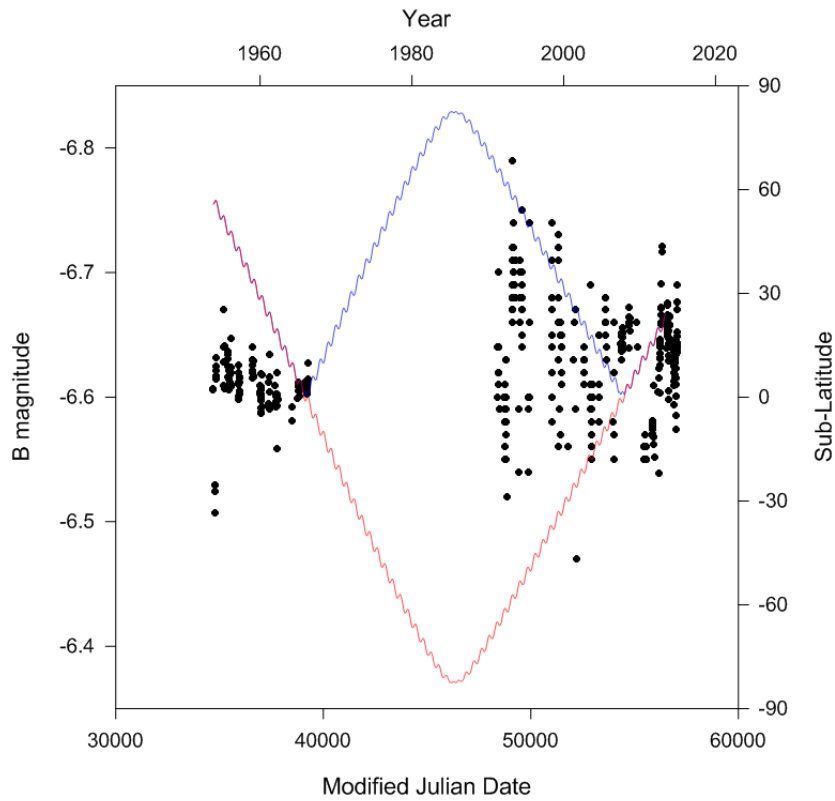


Fig. 4. Brightness variation of Uranus in the B-band between 1953 and 2015. The early data are from Serkowski (1961) and Jerzykiewicz and Serkowski (1966). The uncertainties for the early data are about 0.01 magnitude and for the later data they are a few hundredths of a magnitude. The red line represents the sub-latitude and the blue line is the absolute value of the sub-latitude.

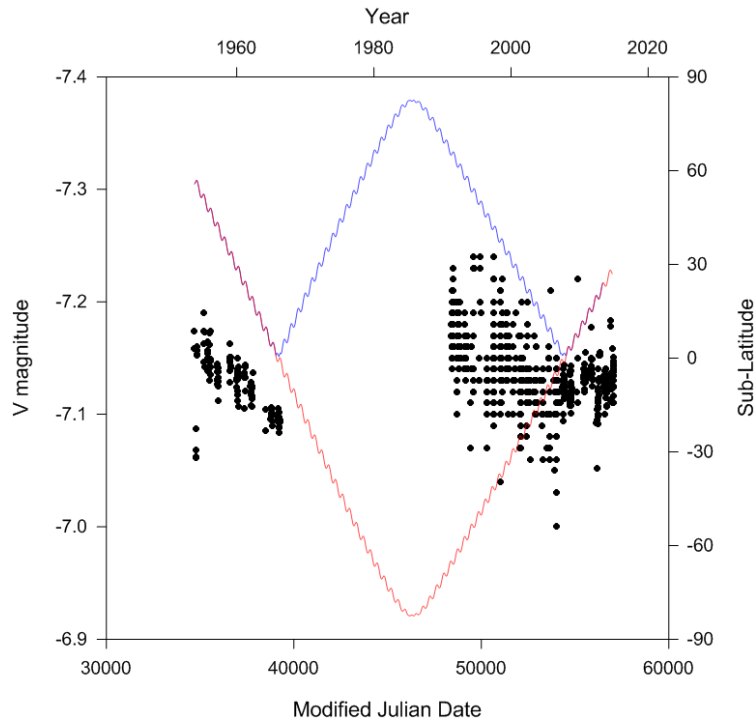


Fig. 5. Same as Fig.4 but for the V-band.

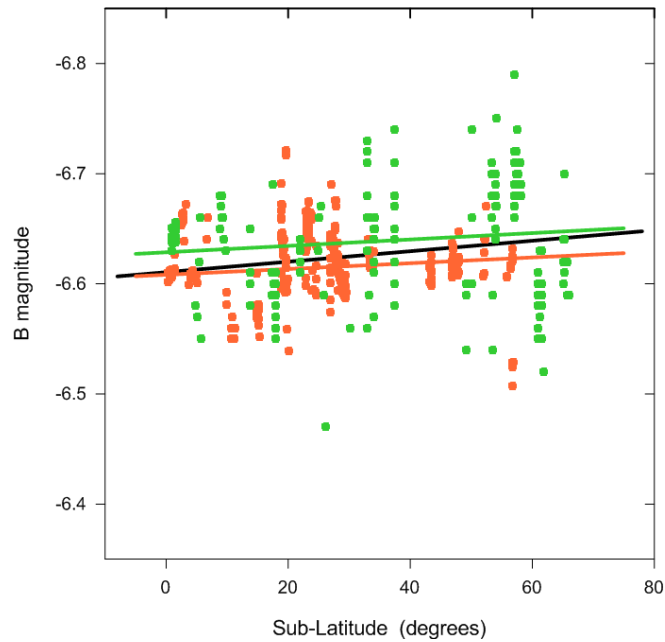


Fig. 6. B-band magnitude as a function of sub-latitude. The black line is the best fit to all the data . The orange and green data and lines are for data where the sub-latitude was north and south of the equator, respectively.

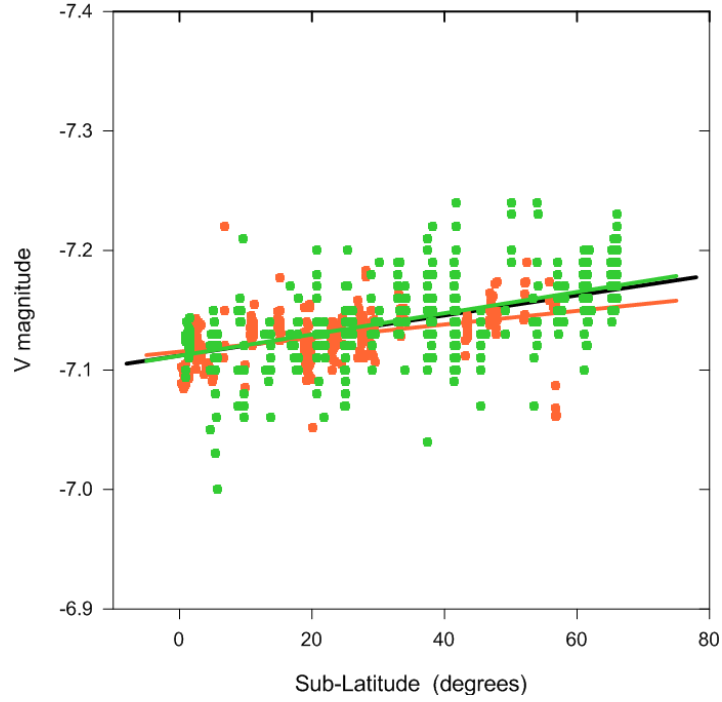


Fig. 7. Same as Fig. 6 but for V-band magnitude.

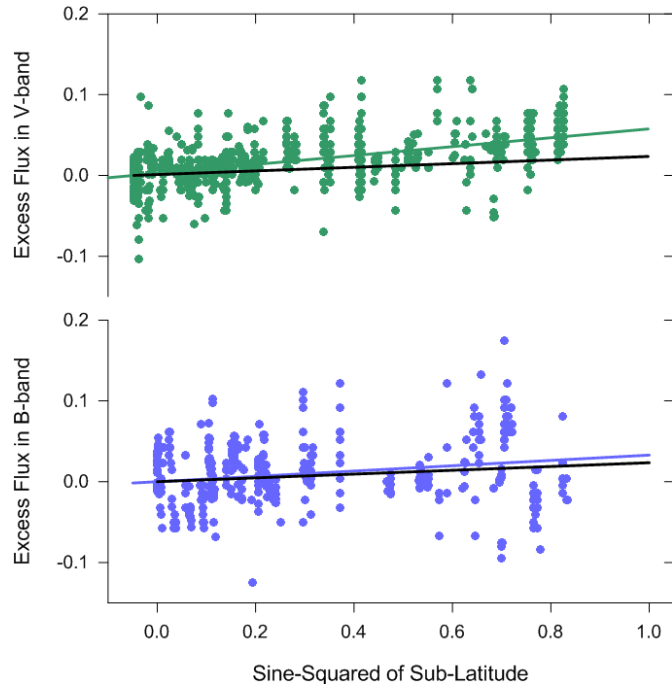


Fig. 8. The excess of flux relative to that at sub-latitude zero is plotted versus the sine-squared of sub-latitude for the B- and V-bands. The black lines represent the corresponding excess of projected surface area due to planetary oblateness.

5. Large brightness variations in the R and I bands

The R- and I-band observations span the years from 1993 through 2014 and include the equinox of 2007. The brightness variations illustrated in Figs. 9 and 10 are much larger than those in B and V. The rate of change of magnitude with sub-latitude is -5.33×10^{-3} magnitudes per degree for the R-band and -2.79×10^{-3} for the I-band, and they correspond with brightness variations measured in tenths of magnitudes (tens of percents).

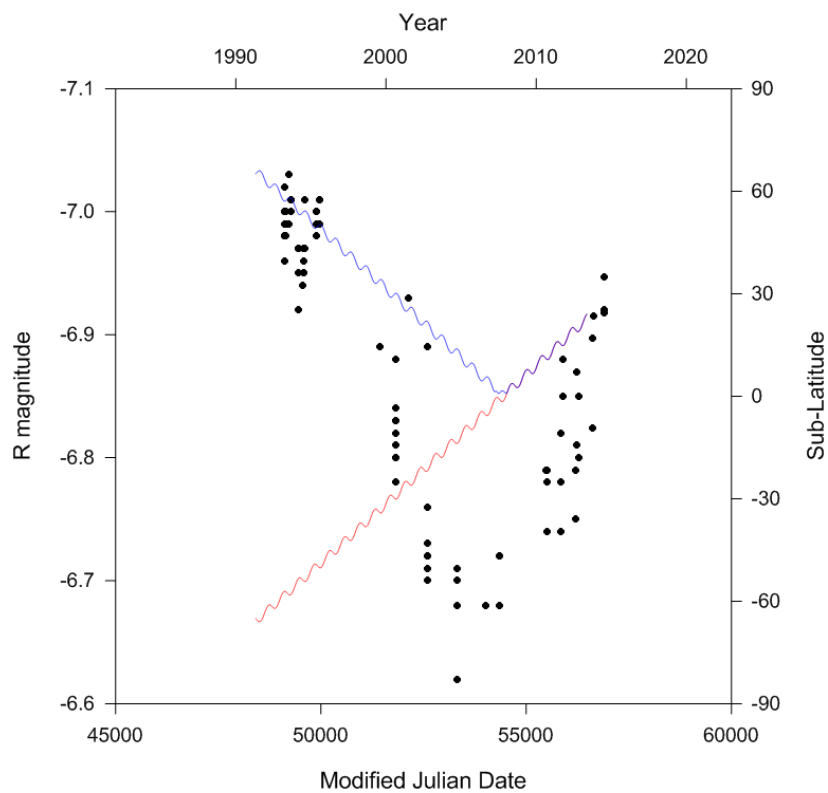


Fig. 9. Brightness variation of Uranus in the R-band between 1993 and 2015. The uncertainties are a few hundredths of a magnitude. The red line represents the sub-latitude and the blue line is the absolute value of the sub-latitude.

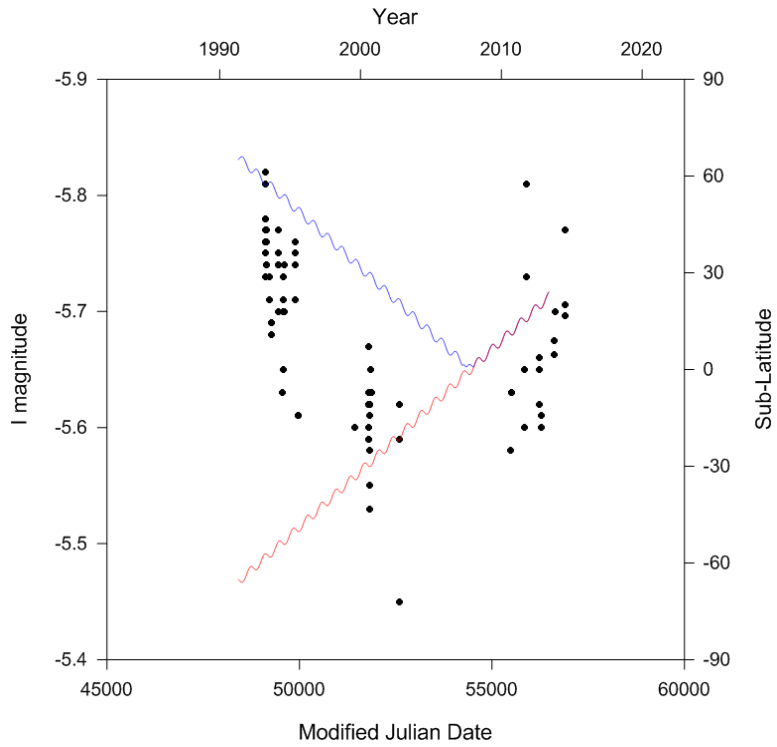


Fig. 10. Same as Fig. 9 but for the I-band.

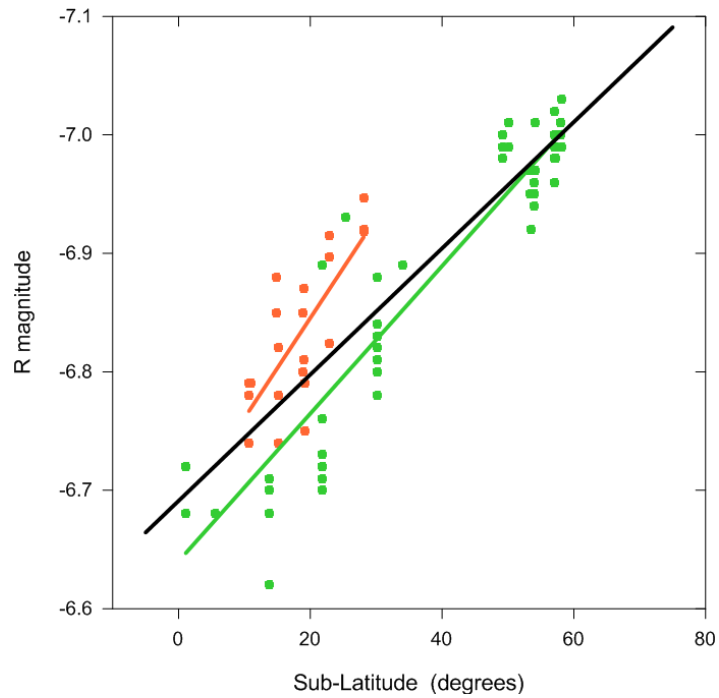


Fig. 11. R-band magnitude as a function of sub-latitude. The black line is the best fit to all the data. The orange and green data and lines are for data where the sub-latitude was north and south of the equator, respectively.

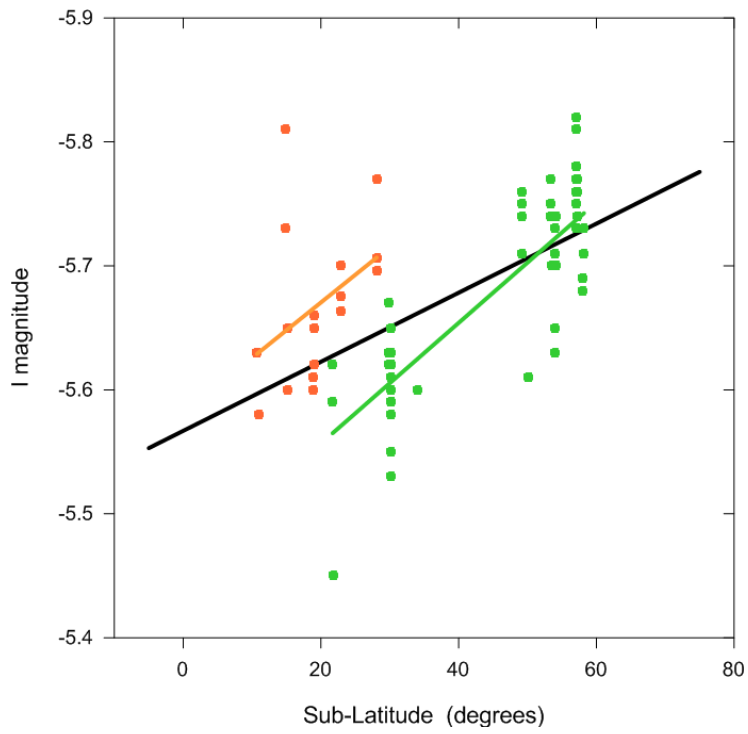


Fig. 12. Same as Fig. 11 but for I-band magnitude.

6. Brightness contributions from the Uranian satellites, rings and clouds

There are several additional factors which could cause observed brightness changes.

Karkoschka (1997) reports albedos for the largest Moons and rings over the 340-910 nm range. In the V filter, Titania is ~2500 times dimmer than Uranus (Astronomical Almanac, 2013). The albedo of Titania divided by that of Uranus is ~0.5 for the V filter but is ~5 for the I filter based the albedos in Karkoschka (1997, 1998). This is a factor of 10 increase and, hence, Titania will still be ~250 times dimmer than Uranus in the I filter. Therefore, Titania will create a negligible ~0.004 magnitude increase when it enters the photometer field of view for the I filter. In rare cases when the phase angle is below 0.1 degree this may rise to 0.01 magnitudes.

The rings are 2000 times fainter than Uranus in visible light (Karkoschka, 1997). The situation is a little different for the I filter. Calculations utilizing the ring dimensions in French et al. (1987) along with the albedos in Karkoschka (2001a) suggest that in the I filter the rings will change the brightness of the Uranus system by ~0.01 magnitude in the I filter.

A third factor, clouds, may create a diurnal brightness change. Karkoschka (2001b) measured the brightness of several clouds at wavelengths between 0.66 and 2.03 μm . Even near equinox when the brighter Northern Hemisphere clouds are less foreshortened, it is unlikely that diurnal variations should exceed 0.01 magnitudes in this study unless there is an unusually large cloud.

7. The polar regions, methane depletion and hemispheric asymmetry

The observed disk-integrated variations of magnitude with latitude are consistent with the characteristic brightness associated with the North and South Polar Regions (NPR and SPR). As early as the 1970s, there was evidence that the planet's SPR was brighter than the surrounding areas in red and near-infrared wavelengths (Price and Franz, 1978 and Radick and Tetley, 1979). Furthermore, Price and Franz report that the polar brightening was much more distinct in 750 nm compared to 619 nm. Twenty years later, HST images show this same trend (Rages et al, 2004). Rages and co-workers also present images taken at 619 nm which show only small brightness changes taking place in the SPR. Images taken in the 890 methane band show little albedo change across the disk (Karkoschka, 1998). One explanation which Rages et al. (2004) propose is the development of clouds of condensed methane over the SPR which later dissipate leaving behind a darker area. This mechanism may also be taking place in the NPR where brightening since 2007 is consistent with higher reflectivity in the northern hemisphere. Infrared images also show bright belts in the Northern Hemisphere (Schmude, 2014).

Methane depletion in the planet's polar regions, as reported by Sromovsky et al (2014), may be associated with the disk-integrated brightness variations we observed as well as the disk-resolved polar brightness discussed above. The weakening of methane absorption bands (which dominate the red and near-IR spectrum) at high latitudes should result in greater reflectivity toward the poles as seen in the R- and I-band results. Conversely, the absence of strong methane bands in the blue and green portions of the spectrum are consistent with the smaller brightness variations recorded in the B and V.

Finally, the observed disparity between brightness in the northern and southern hemispheres agrees fairly well with the asymmetry findings of Karkoschka (2001b). The bottom portion of Karkoscka's Fig. 4 indicates that the southern hemisphere reflects a little more strongly at 430 nm as does our B-band result (Fig. 6). Meanwhile, he finds that the northern hemisphere reflects much more strongly beyond 600 nm which agrees with our R- and I-band results (Figs. 11 and 12). There is a minor disagreement, however, at 550 nm where Karkoscka indicates a slightly brighter northern hemisphere while the V-band data suggests a slightly brighter south (Fig. 7).

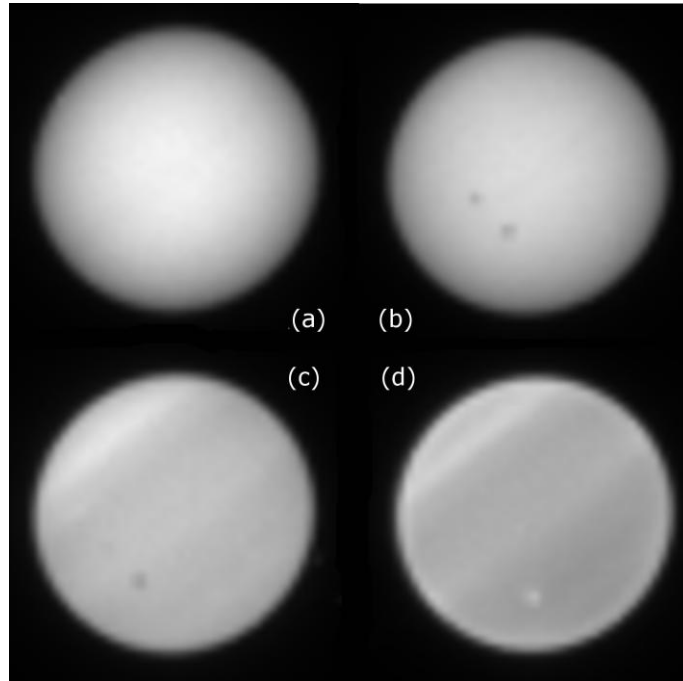


Fig. 13. Uranus is a relatively featureless disk at blue (a) and green (b) wavelengths while the polar regions can be brighter than equatorial latitudes at red (c) and near-IR (d) wavelengths. These HST images were recorded near the time of Uranian equinox on 2007 July 29. The latitude limits of the polar regions have been measured at 44 ± 3 degrees north by Schmude (2014 and 2015a) and 50 ± 0.5 degrees south by Smith 1987). The image names and filters are as follows: a, U9Z70702M, F467M; b, U9Z70503M, F547M; c, U9Z70505M, F658N; and d, U9Z70608M, F850LP.

8. Reference magnitudes, albedos and colors

We adopt the brightness at equinox (zero point numbers in Table 6) as the B, V, R and I reference magnitudes for Uranus. U filter data was also recorded in 2014 by one of us (RWS) when the sub-latitude was +27.0. By applying the slope of ‘magnitude versus sub-latitude’ for the B-band in Table 6, we have arrived at the reference value in Table 7.

Additionally, one of the authors (REB) obtained R_C and I_C magnitudes on the Johnson-Cousins system in 2014. We applied the slope of ‘magnitude versus sub-latitude’ for the R-band in Table 6 to the R_C values and, likewise, applied the I-band slope to the I_C values. The averages of the resulting equinoctial magnitudes were taken as the reference magnitudes in R_C and I_C . These magnitudes are being reported here for the first time.

All reference values are listed in Table 7 along with implied magnitudes at sub-latitude 90 degrees. For comparison, the table also lists U, B and V magnitudes from Karkoschka (1998) and from the Astronomical Almanac. Karkoschka’s B and V magnitudes, which were obtained in July 1995 when the sub-latitude of Uranus was 49 degrees, are toward the bright end of the range from this paper as would be expected given the relatively high latitude. The B and V values from the Almanac lie within the values for 0 – 90 degree sub-latitude from this paper. The U magnitudes from both Karkoschka and from the Almanac are slightly brighter than the range from this paper but there are within the uncertainty.

Table 7. Magnitude summary

	U	B	V	R	R_C	I	I_C
Reference*	-6.28	-6.61	-7.11	-6.69	-6.84	-5.57	-6.00
Uncertainty*	0.05	0.02	0.02	0.02	0.05	0.02	0.05
90 degrees*	-6.32	-6.65	-7.19	-7.17	-7.32	-5.83	-6.25
Uncertainty*	0.05	0.02	0.02	0.03	0.05	0.04	0.05

Almanac**	-6.35	-6.63	-7.19	---	---	---	---
Karkoschka***	-6.36	-6.64	-7.17	---	---	---	---

* This paper

** Astronomical Almanac (2013)

*** Karkoschka (1998) value corresponds to a solar phase angle of 0.7 degree

The geometric albedo is defined as the ratio of the observed flux for a planet to that of a perfectly reflecting Lambertian disk. Taking the V filter as an example, the magnitude of the Sun is -26.75 (Table 8), so the ratio of the luminosity of Uranus (magnitude -7.11 from Table 7) to that of the Sun is 1.39×10^{-8} as shown in Equation 3.

$$L_{\text{ratio}} = 10^{\{(-26.75+7.11)/2.5\}} = 1.39 \times 10^{-8} \quad (3)$$

The average disk radius seen at equinox, r , is 25264 km (including oblateness). The astronomical unit (AU) distance is 149.6×10^6 km, hence there is an area factor, $\sin^2(r/\text{AU})$ or 2.85×10^{-8} .

Therefore the geometric albedo, p , is 0.488 as shown in Equation 4.

$$p = L_{\text{ratio}} / \sin^2(r/\text{AU}) = 0.488 \quad (4)$$

Table 8. Solar magnitudes

U*	B*	V*	R*	R _C **	I*	I _C **
-25.90	-26.10	-26.75	-27.29	-27.15	-27.63	-27.49

* Livingston (2001)
 ** Binney and Merrifield (1998).

The albedo values in Table 9 range from a maximum of 0.561 in the B-band to a minimum of 0.053 in the I-band. This variation is also reflected in the Uranian colors which are described next.

Table 9. Geometric albedos

	U	B	V	R	R _C	I	I _C
Value	0.500	0.561	0.488	0.202	0.263	0.053	0.089
Uncertainty	0.025	0.011	0.010	0.004	0.013	0.001	0.004

The reference colors listed in Table 10 reveal the peculiar spectral energy distribution of Uranus. The planet is moderately red according to the U-B and B-V indices but quite blue according to the indices at longer wavelengths. These unusual colors are due to the strong methane bands which blanket the red and near-IR portions of the spectrum. Table 10 also lists the colors at 60 degrees sub-latitude as inferred from slopes of magnitude versus sub-latitude in Table 1. The B-V and V-R values grow larger which indicates general reddening in the blue-through-red portion of the spectrum. However, the R-I index decreases because the slope of R magnitudes is greater than that of I magnitudes.

Table 10. Colors

	U-B	B-V	V-R	V-Rc	R-I	Rc-Ic
Reference	+0.32	+0.50	-0.42	-0.27	-1.12	-0.84
60 degrees	---	+0.52	-0.15	---	-1.27	---
Uncertainties	0.05	0.02	0.02	0.05	0.02	0.05
Solar values	+0.20	+0.65	+0.54	+0.40	+0.34	+0.34

9. Conclusion

We have reported on brightness changes of Uranus and interpreted them in terms of the planet's geometrical and geophysical properties. Variations in the B- and V-bands were found to be small and in generally good agreement with b- and y-band results reported by Lockwood and Jerzykiewicz (2006). Variations in the R- and I-bands, reported here for the first time, were quite large and are quite interesting. Continued observations, especially at red and near-IR wavelengths are warranted. We also list Uranian reference magnitudes, colors and albedos.

Acknowledgments

RWS thanks the library staff at Gordon State College for their assistance in locating source material used in this study. The data used in Figure 13 was retrieved from the MAST archive of Hubble Space Telescope data at the STScI.

References

- Astronomical Almanac for the Year 2014, 2013. U. S. Govt. Printing Office, Washington DC.
- Binney, J. and Merrifield, M. 1998. Galactic Astronomy. Princeton University Press. Magnitudes referenced at <https://www.astro.umd.edu/~ssm/ASTR620/mags.html>.
- Cousins, A. W. J. 1976a. VRI standards in the E regions. Mem. Roy. Astron. Soc., 81, 25.
- Cousins, A. W. J. 1976b. Standard Stars for VRI Photometry with S.25 Response Photocathodes. Mon. Notes Astron. Soc. Southern Africa, 35,70.
- de Pater, I., Sromovsky, L.A., Fry, P.M., Hammel, H.B., Baranec, C. and Sayanagi, K. 2015. Record-breaking storm activity on Uranus in 2014. Icarus, in press.
- French, R. G., Elliot, J. L., French, L. M. et al 1987. Uranian ring orbits from Earth-based and Voyager occultation observations. Icarus 73, 349-378. [doi:10.1016/0019-1035\(88\)90104-2](https://doi.org/10.1016/0019-1035(88)90104-2).
- Hall, D. S. and Genet R. M. 1988. Photoelectric Photometry of Variable Stars. Willmann Bell, Inc. Richmond, VA.
- Hardie, R.H. 1962. 'Photoelectric Reductions' in Astronomical Techniques (ed. W.A. Hiltner) University of Chicago Press, p. 178.
- Iriarte, B., Johnson, H.L., Mitchell, R.I. and Wisniewski, W.K. 1965. Five-color photometry of bright stars. Sky and Telescope, 30, 21-31.
- Jerzykiewicz, M., Serkowski, K. 1966. The Sun as a Variable Star III. Lowell Observatory Bulletin 6, 295-323.
- Johnson, H.L., Mitchell, R. I., Iriarte, B., and Wisniewski, W. Z. 1966. UBVRJIKL Photometry of the Bright Stars Commun. Lunar Planet. Lab., 4, 99.
- Karkoschka, E. 1997. Rings and satellites of Uranus: Colorful and not so dark. Icarus 125, 348-363. [doi:10.1006/icar.1996.5631](https://doi.org/10.1006/icar.1996.5631).
- Karkoschka, E. 1998. Methane, Ammonia, and Temperature Measurements of the Jovian Planets and Titan from CCD-Spectrophotometry. Icarus 133, 134-146. [doi:10.1006/icar.1998.5913](https://doi.org/10.1006/icar.1998.5913).
- Karkoschka, E. 2001a. Comprehensive photometry of the rings and 16 satellites of Uranus with the Hubble Space Telescope. Icarus 151, 51-68. [doi:10.1006/icar.2001.6596](https://doi.org/10.1006/icar.2001.6596).
- Karkoschka, E. 2001b. Uranus' Apparent Seasonal Variability in 25 HST Filters. Icarus 151, 84-92. [doi:10.1006/icar.2001.6599](https://doi.org/10.1006/icar.2001.6599).

- Livingston, W., 2000. Sun. In: Cox, A.N. (Ed.), *Allen's Astrophysical Quantities*, fourth ed. Springer-Verlag, New York, p. 341.
- Lockwood, G. W. 1978. Analysis of Photometric variations of Uranus and Neptune since 1953. *Icarus* 35, 79-92. [doi:10.1016/0019-1035\(78\)90062-3](https://doi.org/10.1016/0019-1035(78)90062-3).
- Lockwood, G. W. and Thompson, D. T. 1999. Photometric Variability of Uranus, 1972 – 1996. *Icarus* 137, 2-12. [doi:10.1006/icar.1998.6029](https://doi.org/10.1006/icar.1998.6029).
- Lockwood, G.W. and Jerzykiewicz, M. 2006. Photometric variability of Uranus and Neptune, 1950 - 2004. *Icarus*, 180, 442-452. [doi:10.1016/j.icarus.2005.09.009](https://doi.org/10.1016/j.icarus.2005.09.009).
- Lockwood, G. W. and Thompson D. T. 2009. Seasonal photometric variability of Titan, 1972-2006. *Icarus* 200, 616-626. [doi:10.1016/j.icarus.2008.11.017](https://doi.org/10.1016/j.icarus.2008.11.017).
- Mallama, A., Wang, D., Russell, R.A. 2006. Venus phase function and forward scattering from H₂SO₄. *Icarus* 182, 10–22. <http://dx.doi.org/10.1016/j.icarus.2005.12.014>.
- Price, M. J., Franz, O, G. 1978. Limb Brightening on Uranus: The Visible Spectrum, II. *Icarus* 34, 355-373. [doi:10.1016/0019-1035\(78\)90173-2](https://doi.org/10.1016/0019-1035(78)90173-2).
- Radick, R. R., Tetley, W. C. 1979. The 10 February 1977 Lunar Occultation of Uranus. Radius, Limb Darkening, and Polar Brightening at 6900 Å. *Icarus* 40, 67-74. [doi:10.1016/0019-1035\(79\)90053-8](https://doi.org/10.1016/0019-1035(79)90053-8).
- Rages, K. A., Hammel, H. B., Friedson, A. J. 2004. Evidence for temporal change at Uranus' south pole. *Icarus* 172, 548-554. [doi:10.1016/j.icarus.2004.07.009](https://doi.org/10.1016/j.icarus.2004.07.009).
- Schmude, R. W. Jr., 1992. The 1991 apparition of Uranus. *J. Assoc. Lun. & Plant. Obs.* 36, No. 1, pp. 20-22.
- Schmude, R. W. Jr., 1994. The 1992 apparition of Uranus. *J. Assoc. Lun. & Plant. Obs.* 37, No. 3, pp. 116-119.
- Schmude, R. W., Jr. Wideband photometry of Uranus and Neptune in 1993: Preliminary results. *Proceedings of the 43rd convention of the Association of Lunar and Planetary Observers in Las Cruces, NM, August 4-7, 1993, ALPO Monograph No. 1*, pp. 51-63.
- Schmude, R. W. Jr., 1996. Uranus and Neptune in 1993. *J. Assoc. Lun. & Plant. Obs.* 39, No. 2, pp. 63-66.

- Schmude, R. W. Jr., 1997a. Observations of Uranus, Neptune and Pluto in 1994. *J. Assoc. Lun. & Plant. Obs.* 39, No. 3, pp. 127-130.
- Schmude, R. W. Jr., 1997b. The 1995 apparitions of Uranus and Neptune. *J. Assoc. Lun. & Plant. Obs.* 39, No. 4, pp. 181-183.
- Schmude, R. W. Jr., 1998a. The 1996 apparitions of Uranus and Neptune. *J. Assoc. Lun. & Plant. Obs.* 40, No. 3, pp. 121-125.
- Schmude, R. W. Jr., 1998b. Observations of the remote planets in 1997. *J. Assoc. Lun. & Plant. Obs.* 40, No. 4, pp. 167-171.
- Schmude, R. W. Jr., 2000a. Observations of the remote planets in 1998. *J. Assoc. Lun. & Plant. Obs.* 42, No. 1, pp. 13-17.
- Schmude, R. W. Jr., 2000b. Observations of the remote planets in 1999. *J. Assoc. Lun. & Plant. Obs.* 42, No. 4, pp. 158-162.
- Schmude, R. W. Jr., 2001. Observations of the remote planets in 2000. *J. Assoc. Lun. & Plant. Obs.* 43, No. 3, pp. 30-37.
- Schmude, R. W. Jr., 2002. The Uranus, Neptune and Pluto apparitions in 2001. *J. Assoc. Lun. & Plant. Obs.* 44, No. 3, pp. 22-31.
- Schmude, R. W. Jr., 2004. The Uranus, Neptune and Pluto apparitions in 2002. *J. Assoc. Lun. & Plant. Obs.* 46, No. 4, pp. 47-55.
- Schmude, R. W. Jr., 2005. The Uranus, Neptune and Pluto apparitions in 2003. *J. Assoc. Lun. & Plant. Obs.* 47, No. 2, pp. 38-43.
- Schmude, R. W. Jr., 2006a. Uranus, Neptune & Pluto observations during the 2004 apparitions. *J. Assoc. Lun. & Plant. Obs.* 48, No. 2, pp. 41-45.
- Schmude, R. W. Jr., 2006b. The remote planets in 2005-06. *J. Assoc. Lun. & Plant. Obs.* 48, No. 4, pp. 32-37.
- Schmude, R. W. Jr., 2008. The remote planets in 2006-07. *J. Assoc. Lun. & Plant. Obs.* 50, No. 3, pp. 41-45.
- Schmude, R. W. Jr., 2009. ALPO observations of the remote planets in 2007-2008. *J. Assoc. Lun. & Plant. Obs.* 51, No. 2, pp. 41-47.

- Schmude, R. W. Jr., 2010a. ALPO observations of the remote planets in 2008-2009. *J. Assoc. Lun. & Plant. Obs.* 52, No. 2, pp. 43-49.
- Schmude, R. W. Jr., 2010b. ALPO observations of Uranus and Neptune in 2009-2010. *J. Assoc. Lun. & Plant. Obs.* 52, No. 4, pp. 48-50.
- Schmude, R. W. Jr., 2012. ALPO observations of Uranus and Neptune in 2010-2011. *J. Assoc. Lun. & Plant. Obs.* 54, No. 1, pp. 33-38.
- Schmude, R. W. Jr., 2013. ALPO observations of the remote planets in 2011-2012. *J. Assoc. Lun. & Plant. Obs.* 55, No. 4, pp. 41-46.
- Schmude, R. W. Jr., 2014. ALPO observations of the remote planets in 2012-2013. *J. Assoc. Lun. & Plant. Obs.* 56, No. 1, pp. 50-54.
- Schmude, R. W. Jr., 2015a. ALPO observations of the remote planets in 2013-2014. *J. Assoc. Lun. & Plant. Obs.* 57, No. 1, pp. 41-46.
- Schmude, R. W. Jr., 2015b, in preparation.
- Serkowski, K. 1961. The Sun as a variable star II. *Lowell Observatory Bulletin* 5, 157-226.
- Sinnott, R. W., Perryman, M. A. C. 1997. *Millennium Star Atlas*, Sky Publishing Corp., Cambridge, MA.
- Sromovsky, L.A., Karkoschka, E., Fry, P.M., Hammel, H.B., de Pater, I. and Rages, K. 2014. Methane depletion in both polar regions of Uranus inferred from HST/STIS and Keck/NIRC2 observations. *Icarus* 238, 137-155. <http://dx.doi.org/10.1016/j.icarus.2014.05.016>.